

Full-scale simulation study of a generalized Zakharov model for the generation of topside ionospheric turbulence

B. Eliasson

*Department of Physics, Umeå University, SE-901 87 Umeå, Sweden and
Theoretische Physik IV, Ruhr-Universität Bochum, D-44780 Bochum, Germany*

We present a full-scale simulation study of a generalized Zakharov model for the generation of the topside electrostatic turbulence due to the parametric instability during ionospheric heating experiments near the F region peak. The nonlinear tunneling of electromagnetic waves through the ionospheric layer is attributed to multiple-stage parametric decay and mode-conversion processes. At the bottomside of the F region, electrostatic turbulence excited by the parametric instability results in the conversion of the ordinary (O mode) wave into a large amplitude extraordinary (Z mode) wave tunneling through the F peak. At the topside interaction region, the Z mode undergoes parametric decay cascade process that results in the generation of the topside electrostatic turbulence and then conversion process yielding O waves that escape the plasma. This study may explain the observed topside ionospheric turbulence during ground based ionospheric heating experiments.

I. INTRODUCTION

There have been several radar observations of enhanced plasma and ion lines at the topside ionosphere during ground based heating experiments in which the transmitting frequency has been kept somewhat lower than the critical plasma frequency of the F2 layer maximum. A proposed explanation for the observed topside plasma and ion lines is a nonlinear decay of large amplitude Z mode waves, which have been mode converted from the O mode heater wave at the bottomside of the ionosphere, into Langmuir and ion acoustic (IA) waves. The observations have attracted much interest since both the ordinary (O) and fast extraordinary (X) electromagnetic waves are reflected at or below the critical region where $V = 1$, except at a very narrow angular range around the critical angle of incidence (the Spitze angle) where the O mode wave is mode converted to Z mode waves [Budden, 1961; Ginzburg, 1967/1970; Gondarenko *et al.*, 2003; Mjølhus, 1990]. (Throughout the manuscript, we use the standard notation $V = \omega_{pe}^2/\omega^2$, $Y = \omega_{ce}/\omega$ and $U = Y^2$ [Budden, 1961; Ginzburg, 1967/1970] where ω_{pe} is the electron plasma frequency, ω_{ce} is the electron gyrofrequency and ω is the transmitted frequency.) Enhanced topside plasma lines in the F2 region were first observed in heating experiments at Arecibo by Ganguly and Gordon [1983]. During experiments where the EISCAT UHF beam was directed near the Spitze angle, Isham *et al.* [1990] observed enhancements of ion lines in the topside interaction F2 region where $V = 1$. Similar observations at EISCAT were done in the E region by Rietveld *et al.* [2002], where there were no clear dependence of the power of the topside echoes on the power of the plasma turbulence at the bottomside. There are several observations at EISCAT of topside echoes over an angular range of several degrees [Mishin *et al.*, 2001]. In the experiment at EISCAT by Isham *et al.* [1999], which was performed with low duty cycle (200 ms every 10 s), topside excitation of ion and plasma lines were also observed in a angular range of

many degrees from the Spitze angle, including vertical incidence. In order for normally incident O wave to tunnel through the F peak, conversion of the O mode to the Z mode should occur, and the following conditions are necessary. First, that the transmitter frequency should be near the maximum plasma frequency of the F peak so that $V < 1 + Y$ for the peak plasma frequency of the F layer, as discussed by Mishin *et al.* [1997] and shown in the linear E-region simulations for a parabolic density profile [Gondarenko *et al.*, 2003]. Second, the existence of the density/electric field fluctuations within the critical layer, which can occur due to the generation of electrostatic turbulence excited by the parametric instability or in the earlier phase of the nonlinear thermal self-focusing instability [Gondarenko *et al.*, 2006]. Mishin *et al.* [2001] proposed that the topside plasma and ion lines could be due to resonant scatter of the HF pump wave into Z mode waves on the small-scale magnetic field aligned striations, which in turn are created by the HF pump wave via the resonant instability, or, in the case of the low duty cycle experiments with pump frequencies near a multiple of the electron gyro frequency, due to a second-order four wave interaction [Huang and Kuo, 1994]. Rocket observations during heating experiments in Arecibo [Gelinas *et al.*, 2003] revealed Z mode waves and field aligned striations above the O mode reflection point, and evidence of generation of Bernstein waves where the local plasma frequency matches an electron gyro harmonic.

During experiments where the EISCAT UHF beam was directed along the magnetic field lines, Isham *et al.* [1996] discovered spectra with an unusually large spectral width (up to 200 kHz) and a mean frequency shifted by 200-300 kHz away from the heating frequency in both the upshifted and downshifted channels. This feature has been named the HF-induced outshifted line (HFOL). The HFOL spectra come from a height about 3-6 km above the reflection height. Mishin *et al.* [1997] propose that the HFOL feature can be consistently explained if the upper region is the reflection layer of the Z mode ap-

pearing due to the mode conversion at the reflection level of the injected O mode wave. Their scenario includes large-scale density depletions at the Airy maxima of the Z mode, the parametric decay of the Z mode into electron Bernstein and lower hybrid waves [Kuo *et al.*, 1998], and the production of suprathermal electrons by the electrostatic turbulence, which in turn excite Langmuir waves inside the density depletions, yielding the HFOL.

The interaction between the electromagnetic pump wave and the electrostatic turbulence have been modeled with Zakharov-type equations [Kuznetsov, 1974; Zakharov, 1972] and wave kinetic equations [Fejer and Kuo., 1973; Perkins *et al.*, 1974], to understand the wave spectra and radiation generation from electromagnetically driven Langmuir turbulence [DuBois *et al.*, 1991; Galeev *et al.*, 1977; Mjølhus *et al.*, 1995; Stubbe *et al.*, 1992]. In this Letter we analyze the conversion of O mode waves into Z mode waves and the generation of topside ionospheric turbulence numerically with a full-scale simulations of a generalized Zakharov model [Eliasson and Stenflo, 2007] based on a nested grid method [Eliasson, 2007]. We are using realistic length scales and ionospheric parameters relevant for the high-latitude facility EISCAT near Tromsø, Norway, but similar parameters may be also found at high-latitude facilities such as HAARP, Alaska and HIPAS, near Fairbanks, Alaska.

II. MATHEMATICAL MODEL

In our one-dimensional simulation geometry, we assume that a large amplitude electromagnetic wave is injected vertically, along the z axis, into the vertically stratified ionospheric layer. The mathematical model, derived in Eliasson and Stenflo [2007], is based on a separation of time scales, where the time-dependent quantities (here denoted $\psi(z, t)$) are separated into a slow and a high-frequency time scale, $\psi = \psi_s + \psi_h$. The high-frequency component is assumed to take the form $\psi_h = (1/2)\tilde{\psi}(z, t)\exp(-i\omega_0 t) + \text{complex conjugate}$, where $\tilde{\psi}$ represents the slowly varying complex envelope of the high-frequency field, and ω_0 is the frequency of the transmitted electromagnetic wave. Hence the time derivatives on the fast timescale will be transformed as $\partial/\partial t \rightarrow \partial/\partial t - i\omega_0$ when going from the ψ_h variable to the $\tilde{\psi}$ variable. The dynamics of the high-frequency electromagnetic waves and electron dynamics is coupled nonlinearly to the slow timescale electron dynamics via the ponderomotive force acting on the electrons, and is mediated to the ions via the electrostatic field on the slow timescale.

We first present the envelope equations on the fast time scale. The transverse (to the z axis) components of the electromagnetic field in the presence of a slowly varying electron density n_{es} is governed by the electromagnetic

wave equation

$$\frac{\partial \tilde{\mathbf{A}}_{\perp}}{\partial t} = i\omega_0 \tilde{\mathbf{A}}_{\perp} - \tilde{\mathbf{E}}_{\perp}, \quad (1)$$

$$\frac{\partial \tilde{\mathbf{E}}_{\perp}}{\partial t} = i\omega_0 \tilde{\mathbf{E}}_{\perp} - c^2 \frac{\partial^2 \tilde{\mathbf{A}}_{\perp}}{\partial z^2} + \frac{en_{es}\tilde{\mathbf{v}}_{e\perp}}{\varepsilon_0}, \quad (2)$$

where $\tilde{\mathbf{A}}_{\perp}$ and $\tilde{\mathbf{E}}_{\perp}$ is the transverse vector potential (in Coulomb gauge) and electric field, respectively. Here c is the speed of light in vacuum and ε_0 is the electric vacuum permittivity. The z component of the electric field is governed by the Maxwell equation

$$\frac{\partial \tilde{E}_z}{\partial t} = i\omega_0 \tilde{E}_z + \frac{en_{es}\tilde{v}_{ez}}{\varepsilon_0}. \quad (3)$$

The high-frequency electron dynamics is governed by the continuity and momentum equation

$$\frac{\partial \tilde{n}_e}{\partial t} = i\omega_0 \tilde{n}_e - \frac{\partial(n_{es}\tilde{v}_{ez})}{\partial z}, \quad (4)$$

and

$$\begin{aligned} \frac{\partial \tilde{\mathbf{v}}_e}{\partial t} = & i\omega_0 \tilde{\mathbf{v}}_e - \frac{e}{m_e} \left(\hat{\mathbf{z}}\tilde{E}_z + \tilde{\mathbf{E}}_{\perp} + \tilde{\mathbf{v}}_e \times \mathbf{B}_0 \right) \\ & - \hat{\mathbf{z}} \frac{3v_{Te}^2}{n_0} \frac{\partial \tilde{n}_e}{\partial z} - \nu_e \tilde{\mathbf{v}}_e, \end{aligned} \quad (5)$$

respectively, where \mathbf{B}_0 is the geomagnetic field, ν_e is the electron collision frequency, e is the magnitude of the electron charge, m_e is the electron mass, $v_{Te} = (k_B T_e / m_e)^{1/2}$ is the electron thermal speed, k_B is Boltzmann's constant, T_e is the electron temperature, and n_0 is the background electron number density. We have assumed that the ions are immobile on the fast time scale due to their large mass compared to that of the electrons.

The slowly varying electron number density is separated as $n_{es} = n_{e0}(z) + n_s(z, t)$ where $n_{e0}(z) = n_{i0}(z)$ represents the large-scale electron density profile due to ionization/recombination in the ionosphere, and n_s is the slowly varying electron density fluctuations. We regard the electrons as inertialess on the slow time scale, where we also assume quasi-neutrality $n_{is} = n_{es} \equiv n_s$. The dynamics of the ions is governed by the continuity equation

$$\frac{\partial n_s}{\partial t} + n_0 \frac{\partial v_{iz}}{\partial z} = 0, \quad (6)$$

and, since the ions are assumed to be unmagnetized, the slow timescale plasma velocity is obtained from the ion momentum equation driven by the ponderomotive force

$$\frac{\partial v_{iz}}{\partial t} = -\frac{C_s^2}{n_0} \frac{\partial n_s}{\partial z} - \nu_i v_{iz} - \frac{\varepsilon_0}{4m_i n_0} \frac{\partial |\tilde{\mathbf{E}}|^2}{\partial z} \quad (7)$$

where $C_s = [k_B(T_e + 3T_i)/m_i]^{1/2}$ is the IA speed, T_i is the ion temperature, m_i is the ion mass, and we have

denoted $|\tilde{\mathbf{E}}|^2 = |\tilde{\mathbf{E}}_\perp|^2 + |\tilde{E}_z|^2$ and $|\tilde{\mathbf{E}}_\perp|^2 = |\tilde{E}_x|^2 + |\tilde{E}_y|^2$. In obtaining Eq. (7), we have used the ion momentum equation

$$\frac{\partial v_{iz}}{\partial t} = \frac{e}{m_i} E_{zs} - \frac{3v_{Ti}^2}{n_0} \frac{\partial n_i}{\partial z} - \nu_i v_{iz}, \quad (8)$$

together with the electron force balance equation

$$0 = -eE_{zs} - \frac{k_B T_e}{n_0} \frac{\partial n_s}{\partial z} - \frac{\varepsilon_0}{4n_0} \frac{\partial |\tilde{\mathbf{E}}|^2}{\partial z}, \quad (9)$$

where we have neglected effects of the geomagnetic field \mathbf{B}_0 on the ponderomotive force (the $|\tilde{\mathbf{E}}|^2$ -term) since we will consider high-frequency waves with frequencies much higher than the electron gyro-frequency.

III. NUMERICAL SETUP

We next define the simulation setup and physical parameters used in the simulation; the details of the numerical implementation is described in the Appendix of *Eliasson and Stenflo* [2007]. The simulation code uses a one-dimensional geometry, along the z axis. Our simulation box starts at an altitude of 200 km and ends at 400 km. While $\tilde{\mathbf{A}}_\perp$ and $\tilde{\mathbf{E}}_\perp$ are represented on a grid with grid size 2 m everywhere, the rest of the quantities \tilde{n}_e , $\tilde{\mathbf{v}}_e$, n_s , v_{iz} and \tilde{E}_z are resolved with a much denser grid of grid size 4 cm at the bottomside and topside interaction regions, $z = 286.2$ – 287.2 km and $z = 312.8$ – 313.8 km, in order to resolve small-scale structures due to electrostatic turbulence. Outside these regions, all quantities are resolved on the 2-meter grid. This nested grid procedure is used to avoid a severe Courant-Friedrich-Lewy (CFL) condition $\Delta t < \delta z/c$ on the timestep if the electromagnetic field is resolved on the dense grid δz . The ionospheric density profile will be assumed to have a Gaussian shape of the form $n_{i0}(z) = n_{0,max} \exp[-(z - z_{max})^2/10^9]$, where $n_{0,max} = 5 \times 10^{11} \text{ m}^{-3}$ and $z_{max} = 300 \times 10^3 \text{ m}$ are the maximum density and the altitude of the F peak, and $L = 31.6 \times 10^3 \text{ m}$ is the density scale length. The external magnetic field B_0 is set to $4.8 \times 10^{-5} \text{ T}$ and is tilted $\theta = 0.2269 \text{ rad}$ (13°) to the vertical (z) axis so that $\mathbf{B}_0 = B_0[\hat{x} \sin(\theta) - \hat{z} \cos(\theta)]$, which is the case at EISCAT in Tromsø. We assume that the transmitter on ground has been switched on at $t = 0$. The simulation starts at $t = 0.67 \text{ ms}$, when the electromagnetic wave has reached the altitude 200 km. Initially, all time-dependent fields are set to zero, and random density fluctuations of order 10^6 m^{-3} are added to n_s to seed the parametric instability in the plasma. The electromagnetic wave is injected from the bottomside of the simulation box at 200 km, by setting the x component of the electric field to 1 V/m on the upward propagating field (see *Eliasson and Stenflo* [2007]). The transmitter frequency is set to $\omega_0 = 3.66 \times 10^7 \text{ s}^{-1}$, which is somewhat lower than the maximum F peak

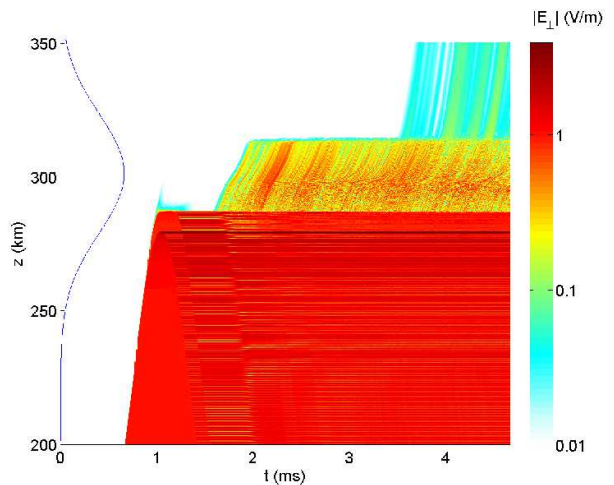


FIG. 1: The amplitude of the perpendicular (to the z axis) electric field in log scale and the density profile of the F layer (solid line). Electrostatic turbulence generated due to the parametric instability at the bottom and top sides of the F layer: at $t \sim 1.7 \text{ ms}$, the O wave is transferred into Z waves which tunnel through the layer, and at $t \sim 3.5 \text{ ms}$, the inverse conversion process yields O waves escaping the plasma.

plasma frequency $\omega_{pe,max} = 3.99 \times 10^7 \text{ s}^{-1}$, calculated with $n_0 = n_{0,max}$. On the other hand, the chosen wave frequency is higher than the maximum Z mode cutoff frequency $\omega_{Z,max} \sim 3.58 \times 10^7 \text{ s}^{-1}$ calculated from $V = 1 + Y$ with $V = \omega_{pe,max}^2/\omega_{Z,max}^2$, $Y = \omega_{ce}/\omega_{Z,max}$, and $\omega_{ce} = eB_0/m_e \approx 8.5 \times 10^6 \text{ s}^{-1}$. By this choice of pump frequency, the O mode is reflected by the overdense plasma layer, while Z mode waves are allowed to propagate to the topside when electrostatic turbulence is generated due to the parametric instability. We use oxygen ions so that $m_i = 16 m_p$ where $m_p = 1836 m_e$ is the proton mass. Further, $T_e = T_i = 1500 \text{ K}$ so that $v_{Te} = 1.5 \times 10^5 \text{ m/s}$ and $C_s = 1.75 \times 10^3 \text{ m/s}$, and we use $n_0 = 3.3 \times 10^{11} \text{ m}^{-3}$, which is the electron number density at $V = 1$. The electron collision frequency is set to $\nu_e = 10^3 \text{ s}^{-1}$ and the effective ion “collision frequency,” due to Landau damping, is set to $\nu_i = 2 \times 10^3 \text{ s}^{-1}$, where we have neglected that the ion Landau damping depends on the wavelength of the IA wave. The value used here is approximately valid for IA waves with wavelengths of ~ 1 – 2 m .

IV. NUMERICAL RESULTS

The time evolution of the electric fields and ion density fluctuations are shown in Figs. 1 and 2 from $t = 0$ to $t = 4.67 \text{ ms}$. Figure 1 shows the spatial and temporal evolution of the perpendicular (to the z axis) electric field amplitude $|\tilde{\mathbf{E}}_\perp| = \sqrt{|\tilde{E}_x|^2 + |\tilde{E}_y|^2}$. After approximately 1 ms, the electromagnetic wave reaches the bottomside interaction for the O mode at $z \approx 287 \text{ km}$ and for the

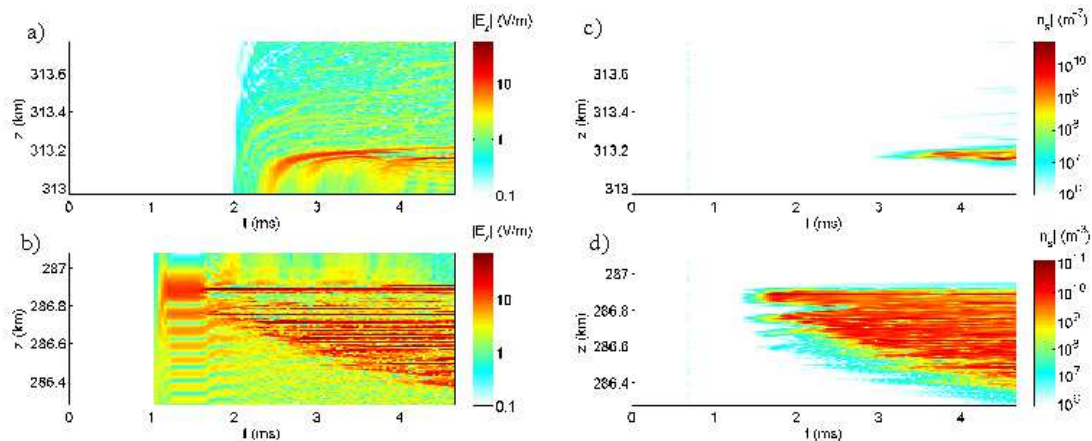


FIG. 2: Electrostatic turbulence generated due to the parametric instability shown with the electric field amplitude E_z at (b) the bottomside and (a) topside interaction regions of the F layer at $t \sim 1.7$ ms and $t \sim 3.5$ ms, respectively. The ion density fluctuation n_s at the interaction regions: (d) the bottomside when large-scale fluctuations are excited due to wave collapse and caviton formation at $t \sim 1.7$ ms and (c) the topside at $t \sim 3.5$ ms.

X mode at a slighter lower altitude $z \approx 270$ km, after which a steady-state standing pattern quickly builds up. At $t \approx 1.6$ ms, there is an efficient conversion of the incident O wave into the Z mode due to rapid development of the density fluctuations (discussed in connection to Fig. 2 below). The Z mode waves propagate from the bottomside at $z = 270$ km to the topside interaction region for the O mode at $z = 312$ km. At $t = 3.5$ ms, we observe excitation of O mode radiation at the topside at $z \approx 312$ km, and these O mode waves propagate away from the ionospheric profile on the topside.

In Fig. 2, we have visualized the \tilde{E}_z component of the high frequency electric field and the ion density fluctuations n_s , in the vicinity of the topside and bottomside interaction regions for the O mode. In Fig. 2(b), we see the arrival of the O mode at the bottom side at $t \approx 1$ ms, after which a standing wave pattern [Ginzburg, 1967/1970] is set up. At $t \approx 1.7$ ms, the standing wave pattern breaks up into small-scale, large amplitude waves. At the same time, seen in Fig. 2(d), large amplitude ion density fluctuations are excited first in the region of the maxima of E_z at $z = 286.75$ km and $z = 286.85$ km (see Fig. 2), and later spreading to lower altitudes. This transition into wave turbulence is closely correlated with the excitation of Z mode waves observed in Fig. 1. At $t = 2$ – 2.5 ms, we see in Fig. 2(a) the arrival of the Z mode at the topside ionosphere. While some weaker waves propagate to higher altitudes, a band of large-amplitude electric field is set up at $z \approx 313.2$ km where the Z mode wave meets the transformation point [Mishin *et al.*, 2001; Mjølhus, 1990] and converts into electrostatic waves. At t later than 3.5 ms the Z mode wave decays into short wavelength Langmuir and IA waves due to a parametric instability, followed by Langmuir wave collapse and ion caviton formation. In Fig 2(c), the ion fluctuations are seen at the topside in a narrow band at 313.2 km. The large amplitude collapsed Langmuir waves and the associated

ion cavitons have sizes of a few tens of centimeters or less and a spacing of a meter or less, similar as in the study of Eliasson and Stenflo [2007]. The topside Langmuir turbulence gives rise to the radiation of O mode waves seen in Fig 1 at $t > 3.5$ ms, in a process described by Mjølhus *et al.* [1995].

V. DISCUSSION

We have performed a simulation study of enhanced topside turbulence, where the transmitter frequency is kept slightly lower than the critical frequency of the F2 layer. Our simulation study reveals that the electromagnetic wave decays parametrically on the bottomside of the ionosphere, in which collapsing wavepackets and ion density depletions are created. This is a three-wave decay of the O mode into one counter-propagating Langmuir (L) wave and one forward scattered IA wave, obeying the matching conditions $\omega_O = \omega_L + \omega_{IA}$ of the frequencies and $k_O = k_L + k_{IA}$ of the wavenumbers, where $\omega_O(k_O)$, $\omega_L(k_L)$ and $\omega_{IA}(k_{IA})$ are given by the O mode, magnetized Langmuir, IA dispersion relation, respectively. A wavelength of the O mode of the order 100 meters leads to wavelengths of the Langmuir and IA waves of the order one meter [Eliasson and Stenflo, 2007]. The linear instability is followed by a rapid Langmuir waves collapse and the generation of ion cavitons. In the nonlinear phase of the instability, there is a strong generation of Z mode waves in the bottomside interaction region. These large-amplitude Z-mode waves are allowed to propagate into the denser plasma to the topside interaction region of the ionospheric layer, where they reach their transformation point and their amplitude increase as their group speed decreases and they are turning into electrostatic waves. At the topside, the Z mode waves undergo a parametric instability into small-scale (few tens of centimeters)

coupled electrostatic and IA waves, followed by Langmuir wave collapse and the formation of ion cavitons. In this last step, Langmuir turbulence generated O mode waves [Mjølhus *et al.*, 1995] are propagating away from the plasma layer on the top side. We note that the wave tunneling and the excitation of topside turbulence occur within a few milliseconds, and may explain the observed topside enhanced plasma and ion lines far away from the Spitz region, in particular during low duty-cycle ionospheric interaction experiments where the impact of iono-

spheric irregularities are minimized [Isham *et al.*, 1999].

Acknowledgments

This work was supported by the Swedish Research Council (VR). Discussions with T. B. Leyser and B. Thidé are gratefully appreciated.

Budden, K. G. (1961), Radio waves in the ionosphere, Cambridge University Press.

Djuth, F. T., M. P. Sulzer, and J. H. Elder (1990), High resolution observations of HF-induced plasma waves in the ionosphere, *Geophys. Res. Lett.*, *17*(11), 1893–1896.

DuBois, D. F., H. A. Rose, and D. Russell (1990), Excitation of strong Langmuir turbulence in plasmas near critical density: Application to HF heating of the ionosphere, *J. Geophys. Res.*, *95*(A12), 21,221.

DuBois, D. F., H. A. Rose, and D. Russell (1991), Coexistence of parametric decay cascades and caviton collapse at subcritical densities, *Phys. Rev. Lett.*, *66*, 1970–1973.

Duncan, L. M., and J. P. Sheerin (1985), High-resolution studies of the HF ionospheric modification region, *J. Geophys. Res.*, *90*(A9), 8371–8376.

Eliasson, B. (2007), A nonuniform nested grid method for simulations of RF induced ionospheric turbulence, *Comput. Phys. Commun.*, *178*, 8–14.

Eliasson, B., and L. Stenflo (2008), Full-scale simulation study of the initial stage of ionospheric turbulence, *J. Geophys. Res.*, *113*, A02305, doi:10.1029/2007JA012837.

Fejer, J. A., and Y.-Y. Kuo (1973), Structure in the nonlinear saturation spectrum of parametric instabilities, *Phys. Fluids*, *16*, 1490, doi:10.1063/1.1694546.

Galeev, A. A., R. Z. Sagdeev, V. D. Shapiro, V. I. Shevchenko (1977) Langmuir turbulence and dissipation of high-frequency energy, *Sov. Phys. JETP*, *46*, 711–720.

Ganguly, S., and W. E. Gordon (1983), Heater enhanced topside plasma line, *Geophys. Res. Lett.*, *10*(10), 977–978.

Gelinas, L. J., M. C. Kelley, M. P. Sulzer, E. Mishin, M. J. Starks (2003), In situ observations during an HF heating experiment at Arecibo: Evidence for Z-mode and electron cyclotron harmonic effects, *J. Geophys. Res.*, *108*(A10), 1382, doi:10.1029/2003JA009922.

Ginzburg, V. L., *Rasprostranenie Elektromagnitnykh Voln v Plazme* (The Propagation of Electromagnetic Waves in Plasmas) 2nd ed. (Moscow: Nauka, 1967) [Translated into English (Oxford: Pergamon Press, 1970)].

Gondarenko, N. A., P. N. Guzdar, S. L. Ossakow, and P. A. Bernhardt (2003), Linear mode conversion in inhomogeneous magnetized plasmas during ionospheric modification by HF radio waves, *J. Geophys. Res.*, *108*(A12), 1470,

doi:10.1029/2003JA009985.

Gondarenko, N. A., S. L. Ossakow, and G. M. Milikh (2006), Nonlinear evolution of thermal self-focusing instability in ionospheric modifications at high latitudes: aspect angle dependence, *Geophys. Res. Lett.*, *33*, L16104, doi:10.1029/2006GL025916.

Huang, J., and S. P. Kuo (1994), Cyclotron harmonic effect on the thermal oscillating two-stream instability in the high latitude ionosphere, *J. Geophys. Res.*, *99*(A2), 2173–2181.

Isham, B., W. Kofman, T. Hagfors, J. Nordling, Bo Thidé, C. LaHoz, and P. Stubbe (1990), New phenomena observed by EISCAT during an RF ionospheric modification experiment, *Radio Sci.*, *25*(3), 251–262.

Isham, B., C. La Hoz, H. Kohl, T. Hagfors, T. B. Leyser, and M. T. Rietveld (1996), Recent EISCAT heating results using chirped ISR, *J. Atmos. Terr. Phys.*, *58*, 369–383.

Isham, B., B. T. Rietveld, T. Hagfors, C. La Hoz, E. Mishin, W. Kofman, T. B. Leyser, and A. P. Van Eyken (1999), Aspect angle dependence of HF enhanced incoherent backscatter, *Adv. Space Res.* *24*(8), 1003–1006.

Kuo, S. P., E. Koretzky, and M.C. Lee (1998), Parametric excitation of lower hybrid waves by Z-mode waves near electron cyclotron harmonics at Tromsø, *J. Geophys. Res.*, *103*(A10), 23,373–23,379.

Kuznetsov, E. A. (1974), The collapse of electromagnetic waves in a plasma, *Sov. Phys. JETP*, *39*, 1003–1007. [*Zh. Eksp. Teor. Fiz.*, *66*, 2037.]

Mishin, E., T. Hagfors, and W. Kofman (1997), On origin of outshifted plasma lines during HF modification experiments, *J. Geophys. Res.*, *102*(A12), 27,265–27,269.

Mishin, E., T. Hagfors, and B. Isham (2001), A generation mechanism for topside enhanced incoherent backscatter during high frequency modification experiments in Tromsø, *Geophys. Res. Lett.*, *28*(3), 479–482.

Mjølhus, E. (1990), On linear conversion in a magnetized plasma, *Radio Sci.*, *20*, 1321–1339.

Mjølhus, E., A. Hanssen, and D. F. DuBois (1995), Radiation from Electromagnetically Driven Langmuir Turbulence, *J. Geophys. Res.*, *100*(A9), 17,527–17,541.

Perkins, F. W., C. Oberman, and E. J. Valeo (1974), Parametric instabilities and ionospheric modification, *J. Geophys. Res.*, *79*(10), 1478–1496.

Rietveld, M. T., B. Isham, T. Grydeland, C. La Hoz, T. B. Leyser, F. Honary, H. Ueda, M. Kosch, and T. Hagfors (2002), HF-pump-induced parametric instabilities in the auroral E-region, *Adv. Space Res.*, *29*(9), 1363–1368.

Stubbe, P., H. Kohl, and M. T. Rietveld (1992), Langmuir

turbulence and ionospheric modifications, *J. Geophys. Res.*, *97*(A5), 6285–6297.

Zakharov, V. E. (1972), Collapse of Langmuir waves, *Sov. Phys. JETP, Engl. Transl.*, *35*, 908–912.